17th World Conference on Earthquake Engineering, 17WCEE
Sendai, Japan - September 13th to 18th 2020

MATERIAL TESTING INTEGRATED SIMULATION FOR RC STRUCTURE REHABILITATED WITH SHAPE MEMORY ALLOYS

D. Jung[(1)] and B. Andrawes[(2)]

[(1)] *Assistant Professor, Pusan National University, djung@pusan.ac.kr*
[(2)] *Professor, University of Illinois at Urbana-Champaign, andrawes@illinois.edu*

Abstract

There has been a great deal of interest in developing new, innovative construction materials that can compensate for weaknesses of conventional materials. In order to assure the structural safety and durability of the new materials during the life span of civil infrastructure, it is important to thoroughly study and predict behavior of the new materials under severe loading and rapid-changing environmental conditions. This paper studies the development and application of a new simulation framework for studying responses of structural systems equipped with unconventional materials under extreme loading conditions. The new hybrid (experimental-numerical) simulation method, named material testing integrated (MTI) simulation is able to extract the complex behavior of physical materials, and conduct numerical simulation of full structural systems. The concept of MTI simulation can be applied to predict flexural response of reinforced concrete (RC) columns with a high focus on compressive behavior of concrete. This application is based on two assumptions: 1) overall flexural response of the RC columns is approximated by using fiber-based beam-column elements, and 2) complex behavior of concrete expected in localized regions of the columns (i.e. plastic hinge) is provided from physical concrete specimens. The MTI simulation framework used in this study consists of four key components: 1) main simulation coordinator which controls overall simulation process, 2) structural analysis platform capable of constructing hybrid models of a structural system and predicting its responses, 3) experimental test setup which includes a load-carrying device and its control system, and 4) experimental data storage which collects and processes experimentally obtained material behaviors. One of the great advantages of MTI simulation is that this method can capture realistic material behavior from physical specimens (concrete cylinders in this case) that may not be accurately predicted by existing material models, and directly use it in numerical simulation. Much higher simulation accuracy is expected, compared to purely numerical simulation. Because only the material of special interest is fabricated in small-unit scale and tested under desired conditions, there is no need for using complex and expensive experimental test setup. The use of small unit specimens will also allow easy application of various material-related parameters or loading conditions, reflecting a variety of situations. This feature is expected to make structural performance evaluations more cost-effective and flexible. In this study, the new simulation method is employed to explore structural cyclic response of RC frame rehabilitated with external shape memory alloy (SMA) spirals that apply active confinement on concrete. One example simulation was carried out to evaluate the performance of SMA confinement on the lateral cyclic response of the frame when SMA spirals are applied to repair damaged regions of the frame. Simulation results revealed that the damaged RC frame continued to maintain its lateral force capacity after being repaired with the SMA spirals.

Keywords: hybrid simulation, shape memory alloys, active confinement, pre-existing damage, temperature variations

1. Introduction

A wide range of new, innovative construction materials have been continuously developed and studied for civil engineering applications [1-7]. Despite their distinguished characteristics, the possibility exists that some materials exhibit unexpected behaviors or degraded functionality when exposed to high temperature variations, chemical reactions, and repeated and/or sustained loads [8-12]. In order to properly evaluate performance of a structure equipped with the novel materials, it is crucial to thoroughly study how those materials behave in the rapidly varying conditions and how the changed material behavior can affect responses of the structure both at component and system levels.

The task of evaluating structural performance, taking into account such complex conditions, however, could be difficult and costly to achieve with conventional approaches. Although many sophisticated computer-based structural simulations have become available, unique material behaviors and multi-physical phenomena under such complex conditions may not be properly reflected in the simulations. On the other hand, large-scale experiments [13-17] enable accurate and reliable structural performance evaluation. However, test setups with diverse loading effects are not readily available, and cost and time to construct large test specimens can be substantial.

In this study, a new type of simulation framework, named material testing integrated (MTI) simulation [18], is adopted. This approach takes advantages of both numerical simulation and experimental testing. It captures realistic material behaviors through physical material testing and uses them directly in the numerical simulation of a full-scale structural system. MTI simulation is well suited to explore behaviors of new materials and their implications on the overall structural responses. This study presents MTI simulation of a reinforced concrete (RC) frame structure rehabilitated with shape memory alloys (SMAs), a class of smart materials with distinct thermo-mechanical properties [19].

2. Material Testing Integrated (MTI) Simulation

2.1 Conceptual discussion

MTI simulation focuses on the behavior of individual material which has a crucial impact on the system-level structural response. Local material behaviors are extracted experimentally from a sample specimen and provided for the prediction of a global structural response. MTI simulation can be considered as a type of hybrid simulation [20-23] in that the entire structure is divided into analytical and experimental domains at the material level, and that responses of the two domains are combined as a whole. Compared to the conventional hybrid simulation, MTI simulation can be used as a more cost-effective and flexible method of structural performance evaluation. Without fabricating large specimens, small-scale specimens of particular materials can be tested, using a simple test setup, and be readily replaced for subsequent tests. Fig. 1 illustrates the concept of MTI simulation.

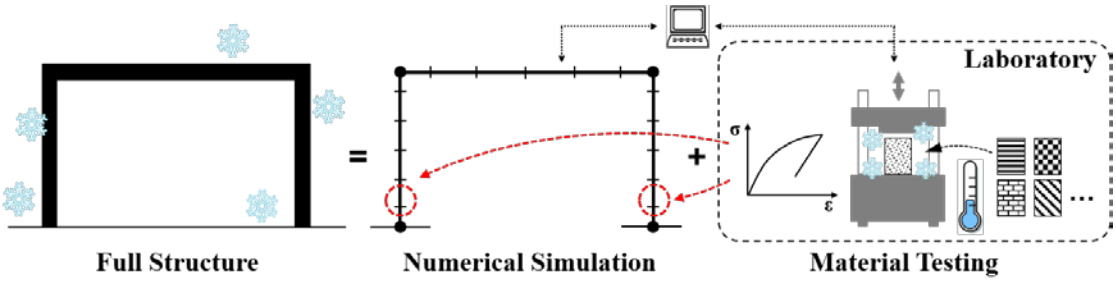

Fig. 1 – Concept of MTI simulation

The concept of MTI simulation can be used to assess responses of flexural-dominant RC columns with special attention to compressive behavior of concrete. Two underlying assumptions are: 1) the flexural

© The 17th World Conference on Earthquake Engineering

columns are numerically modeled by using fiber-based beam-column elements, and 2) complex material behaviors exist in limited regions of a column such as plastic hinges. Fig. 2 depicts how the fiber-based section analysis is carried out in conjunction with physical material testing. If axial strain (ε_a) and curvature (κ) at a plastic hinge region (Section 1) are numerically calculated, strain (ε_i) of each i_{th} concrete fiber is also calculated (Eq. 1), assuming that the section remains plane after bending. Once the highest compressive strain demand (ε_{max}) is selected, a concrete cylinder in laboratory is deformed by a corresponding axial deformation. Measured stress-strain data will construct a new uniaxial constitutive relationship of concrete in the plastic hinge region. Axial force (N) and bending moment (M) at Section 1 are calculated from the experimental concrete stress (σ_i) on each fiber area (A_i) and numerical steel bar stresses (Eq.2 and 3).

$$\varepsilon_i = \varepsilon_a - y_i\kappa \qquad i = 1, 2, 3, \ldots n \tag{1}$$

$$N = \Sigma\,(\sigma_i A_i) \tag{2}$$

$$M = \Sigma\,(-y_i \sigma_i A_i) \tag{3}$$

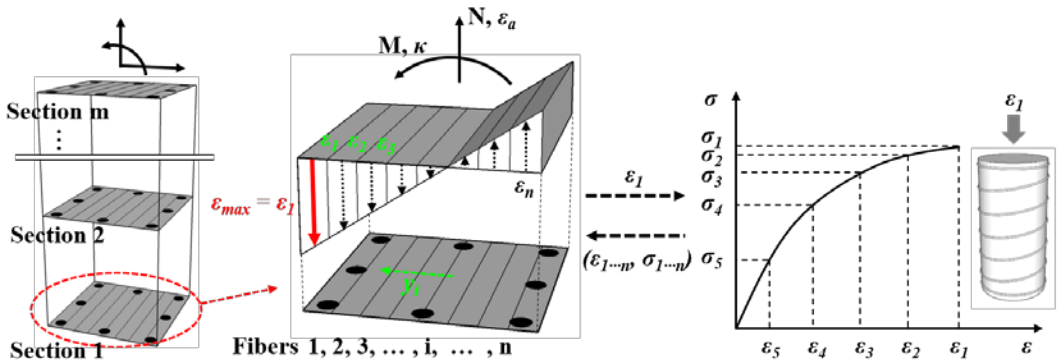

Fig. 2 – Determination of section response within a flexural RC member, using experimental testing of a concrete cylinder

2.2 Simulation framework

For implementation of the MTI simulation concept, a new framework with various components was established. The components used in this study include: 1) main simulation coordinator which controls overall simulation process, 2) structural analysis platform capable of constructing hybrid (numerical-experimental) models of a structural system, 3) experimental test setup which includes a load-carrying device and its control system, and 4) experimental data storage which collects and processes experimentally obtained material behaviors. The composition of the simulation framework and data flow are illustrated in Fig. 3.

The main simulation coordinator administers overall simulation process by providing global displacements that will be imposed on the structural system. The target displacements (command) are sent to the structural analysis platform, and restoring forces (feedback) were returned to the coordinator at each simulation step. In this study, the coordinator developed in LabVIEW sent target displacements for the RC frame subjected to quasi-static lateral loading. For communication of command and feedback, Transmission Control Protocol/Internet Protocol (TCP/IP) network was used.

© The 17th World Conference on Earthquake Engineering

For the structural analysis platform, a new software program was developed in MATLAB. This program contains a base numerical model of the structural system and performs non-linear finite element analysis (FEA). The RC frame which consisted of flexibility-based beam-column elements [24, 25] was used as the base model. In the program, the strain demand on the concrete fibers are sent to the load-carrying device in laboratory as command. The numerical model becomes hybrid (numerical-experimental) as feedback (i.e. experimental stress-strain relationships) are integrated into the model as depicted in Fig. 2.

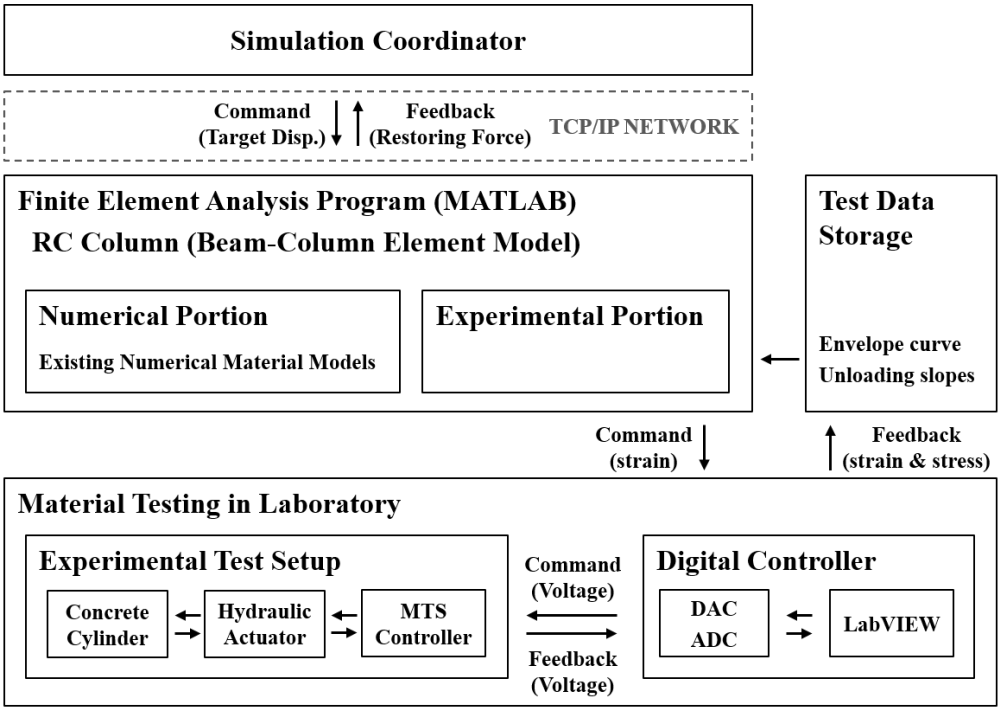

Fig. 3 – Schematic diagram of MTI simulation framework conducted with concurrent material testing

Digital controller is an interface program between the MATLAB FEA program and the experimental test setup. It was newly developed in LabVIEW to control uniaxial motions of the load-carrying device (hydraulic actuator) which applies axial deformation to the concrete specimen. The program operates a hardware device that acts as digital-to-analog and analog-to-digital converters (DAC and ADC). Digital command from the MATLAB FEA program is converted into analog voltage signal, and this voltage signal is fed into an analog controller (MTS controller) controls hydraulic servo valves of the actuator. For precise motion control and smooth movement of the actuator, Ramp-Hold phase algorithm proposed by Nakata et al. [26] was implemented.

The raw displacement-force responses measured from the concrete specimen are preprocessed and stored into two key material properties: 1) envelope of the stress-strain curve and 2) unloading slopes. The envelope curve provides a common compressive behavior path for all concrete fibers, and the unloading slopes are used to describe hysteresis loops of individual fiber unloaded from the envelope curve. Fig. 4 shows how the two properties are obtained from cyclic behaviors of concrete. In Fig. 4a, data points on path O-A-C-D constitute the envelope curve whereas the unloading slopes are estimated from points on paths A-B and D-E. To reflect changes in the unloading slopes under each unloading strain (ε_{UNL}), the entire stress range is divided into several sections (e.g. Section 1 throughout Section b in Fig. 4b), and averaged unloading slope (e.g. E_{11}) is obtained at each stress section. This modeling scheme is implemented whenever a new datum point added during the simulation.

© The 17th World Conference on Earthquake Engineering

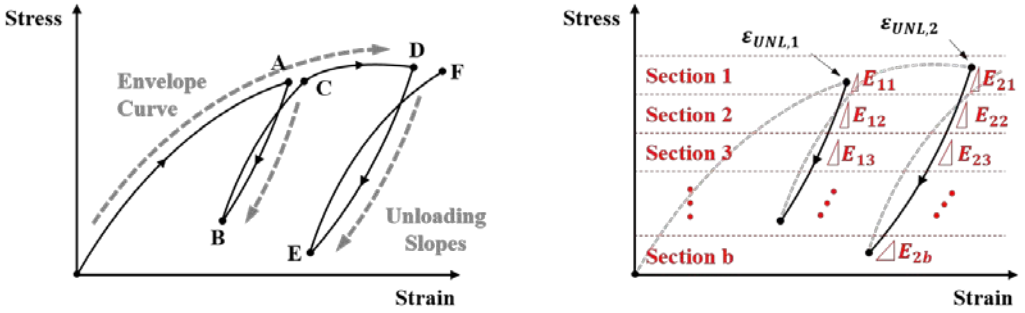

(a) (b)

Fig. 4 – Construction of a new uniaxial constitutive relationships of concrete

3. Active Confinement Technique using Shape Memory Alloys

SMAs have been known as a smart engineering material, and their applications in civil engineering have been extensively studied [2, 3, 5-7, 27, 28]. One of the recent applications of SMA is active confinement technique which uses strong pre-stressing force for concrete confinement. Compared to passively confined concrete which relies on lateral dilation of concrete, actively confined concrete exhibits much higher force deformation capacities under compression. The principle behind the SMA-active confinement technique is shape memory effect of SMA associated with the phase transition of crystal structure at elevated temperature. At a temperature below the martensite finish temperature (M_f), the SMA is in martensite phase and can be permanently deformed after being unloaded from large deformation. If it is heated above austenite start temperature (A_s), austenite phase begins to form and causes the SMA to recover its original shape until the austenite finish temperature (A_f) is reached. High recovery stress (pre-stressing force) can be exerted when this shape recovery is restrained.

Andrawes and Shin [32] and Shin and Andrawes [5] implemented the active confinement technique using NiTiNb SMA wires for seismic retrofitting of RC columns with insufficient lateral confinement. SMA wires prestrained by 6% are spirally applied around plastic hinges of the RC columns and firmed anchored. If the SME of the SMA wires are thermally triggered, the SMA wires unable to recover their original shape develop high pre-stressing force, and actively confine the plastic hinge regions. Fig. 5 illustrates the application of the SMA confinement to the RC columns. The efficacy of the SMA confinement to improve structural performance of RC members has been validated in many previous experimental and numerical studies [5, 29-35]. However, more research is still needed on how the SMA confinement would work under varying ambient temperature and how it affects the behavior of damaged concrete in repair of concrete structures.

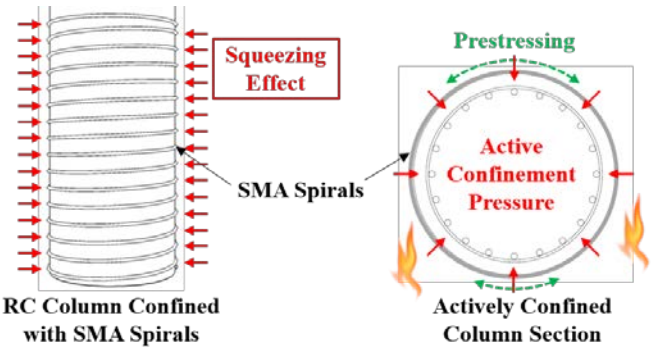

Fig. 5 – Application of active confinement to a RC column using SMA spirals

© The 17th World Conference on Earthquake Engineering

4. Application Example of MTI Simulation

As an exploratory study that demonstrates the capabilities of MTI simulation, this paper presents an example MTI simulation conducted for a simple RC frame structure repaired with SMAs, a scenario which could not be readily reflected in traditional simulation approaches.

4.1 Description of RC frame

Fig. 6 shows a configuration of the RC frame structure considered in this study. Two circular RC columns which had a 9.75 m height and a 1.22 m diameter supported a 39 m long rigid beam. Monolithic connections and fixed boundary conditions were assumed at the top and base of the columns, respectively. The columns were reinforced with eighteen No. 11 longitudinal steel bars. No. 4 (12.7 mm) internal steel hoops were placed at a 305 mm spacing, providing insufficient lateral confinement. Each column had an axial force of 3864 kN (10% of the columns' force capacity). The frame was assumed to be subjected to quasi-static lateral displacement, forming plastic hinges at the top and base of the columns.

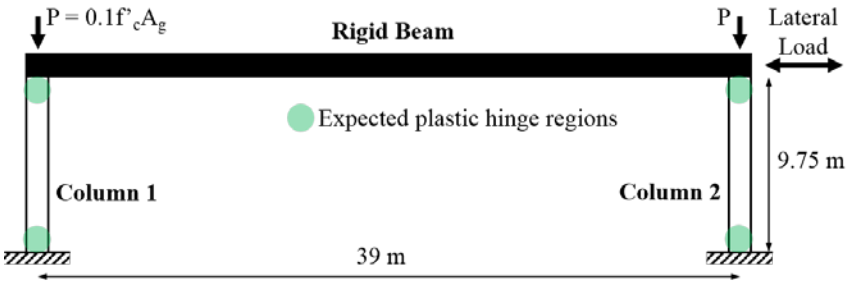

Fig. 6 – Layout of the RC frame structure used in this study

A base numerical model of the frame was first developed in the MATLAB FEA program. Fig. 7 shows numerical modeling of the RC columns represented by single flexibility-based beam-column element with four Gauss-Lobatto integration points (IPs). The top and bottom integration points (i.e. IP_4 and IP_1) were assumed to describe flexural responses of the plastic hinge regions. For the fibers of longitudinal steel bars, Giuffrè-Menegotto-Pinto model [36, 37] was used with 200 GPa Young's modulus, a 414 MPa yield strength and strain hardening ratio of 1%. Both numerical and experimental uniaxial material models were employed for concrete fibers depending on their confinement effects. Details of concrete materials will be discussed in the example section.

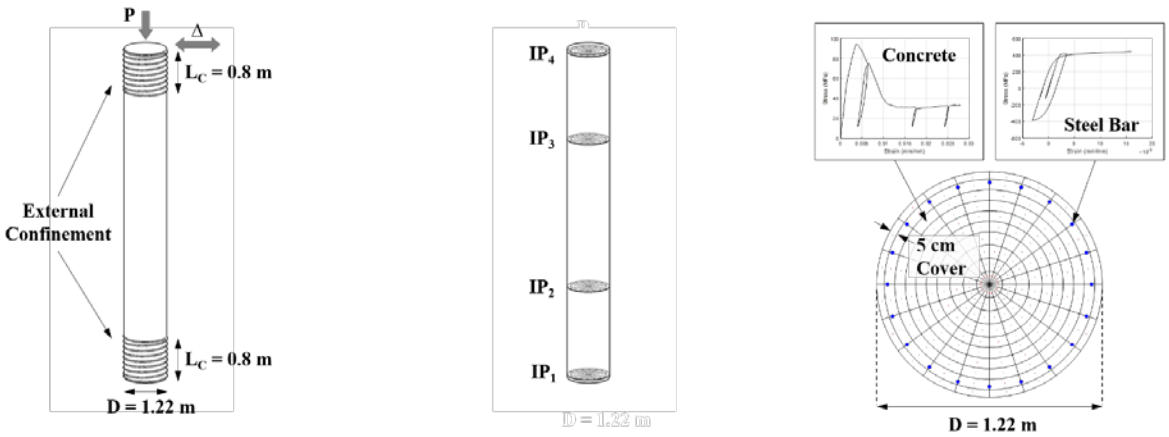

(a) (b) (c)

Fig. 7 – Numerical modeling of the flexural RC column members: (a) RC column with external SMA confinement, (b) beam-column element model and (c) composite fiber section with uniaxial material behaviors

© The 17th World Conference on Earthquake Engineering

4.2 Test set-up for MTI simulation

Fig. 8 shows physical setup of the MTI simulation framework (see Fig. 3). All the software programs including the simulation coordinator, the MATLAB FEA program and the LabVIEW digital controller were executed in a single laptop computer. An USB type National Instruments data acquisition (NI-DAQ) device was used as the DAC and ADC hardware, connecting the digital controller and the analog controller (MTS controller). A 445 kN capacity servo-controlled hydraulic load frame was used to apply uniaxial compressive loading to a concrete cylinder. The concrete cylinder (102 × 203 mm) had an average compressive strength of 32.4 MPa. The specimen was provided with SMA wires to represent actively confined concrete in the columns. Table 1 shows diameter, spacing and recovery stress of the SMA wires designed to apply active confinement pressure of 1.38 MPa after heating [29]. An external LVDT and a load cell were used to measure axial displacement and force feedback of the specimen, respectively.

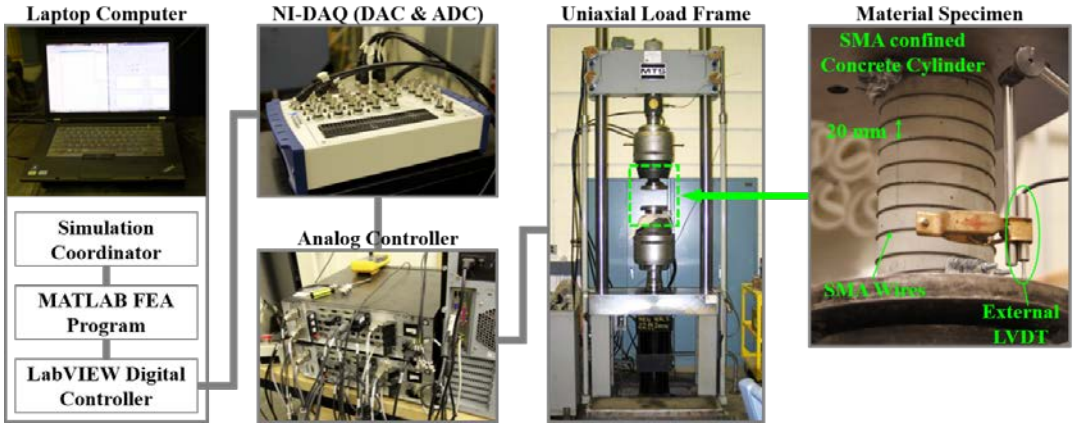

Fig. 8 – Simulation framework and test setup for MTI simulation used in this study

Table 1 – Specifications of the SMA confinement

Wire diameter	Wire spacing	Recovery stress	Confining pressure
1.9 mm	20 mm	551 MPa	1.38 MPa

4.3 Simulation scenario – Pre-existing damage effect

The objective of the simulation was to investigate the effect of SMA repair on the damaged concrete. If a RC structure is damaged from a foreshock earthquake, an emergency repair strategy using SMA confinement [34, 38] can be implemented to avoid more significant damages or total failure of the structure under sequential earthquakes.

The simulation was carried out in two phases according to a loading protocol shown in Fig. 9. In Phase 1, the as-built (i.e. without SMA confinement) RC frame (see Fig. 6) was laterally deformed by 1.2% drift ratio to mimic the initial seismic damage effect, and returned to a zero lateral force position. Two concrete materials were used for modeling of the columns (see Fig. 7) in Phase 1: 1) unconfined (cover) concrete and 2) core concrete confined by the internal steel hoops. For the numerical modeling of cover concrete, the Popovics concrete model [39] with a compressive strength of 32.4 MPa at a strain of 0.2% and zero tensile strength was chosen. For the core concrete, on the other hand, experimental data extracted from the concrete cylinder was used. The concrete cylinder was tested without activation of the SME in Phase 1, assuming that the inactivated SMA wires can apply the low level passive confinement effect of the steel hoops. The concrete materials used in Phase 1 are shown in Fig. 10a.

© The 17th World Conference on Earthquake Engineering

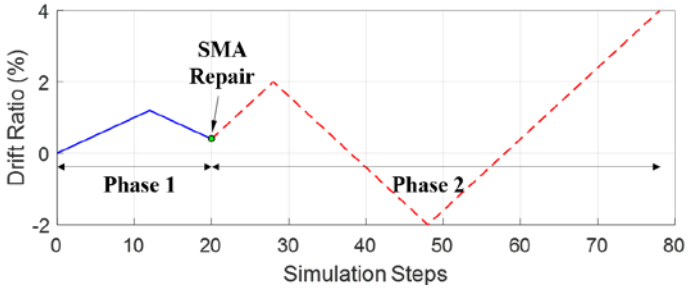

Fig. 9 – Lateral loading protocol for the frame structure

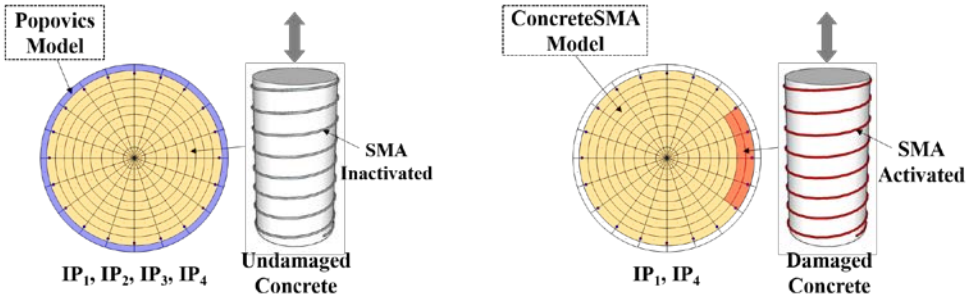

(a) (b)

Fig. 10 – Concrete materials used for the RC columns: (a) Phase 1 and (b) Phase 2

The Phase 1 simulation was expected to induce partial spalling of cover concrete and minor damages in core concrete at the top and bottom (IP_1 and IP_4) of the columns. After Phase 1, the frame was provided with SMA confinement in the damaged regions for the repair, and subjected to the lateral loading up to 4% drift ratio in Phase 2 (see Fig. 9), which corresponded to the greater earthquake loading. To mimic the SMA repair effect, the concrete cylinder tested in Phase 1 was heated, and tested again in Phase 2 to supply a new compressive behavior for the repaired core concrete at IP_1 and IP_4 (see Fig. 10b). The damages of core concrete fibers which did not reach the peak compressive stress in Phase 1 were considered negligible. For those undamaged, actively confined concrete fibers, a uniaxial concrete model, ConcreteSMA [40, 41] which describes the compressive behavior of SMA confined concrete, was implemented. The concrete materials in the middle fiber sections (IP_2 and IP_3) and the steel materials in all fiber sections remained unchanged during Phase 2.

Fig. 11depicts how the concrete behaviors between Phase 1 to Phase 2 are connected, which is crucial for continuous transition of the material behaviors. As an example, the last stress-stain point (Point C) reported during unloading in Phase 1 becomes a starting point in Phase 2. For this curve to be engaged in again compression following the new concrete behavior (B-D) in Phase 2, it needs to be loaded beyond Point B which had zero stress in Phase 1.

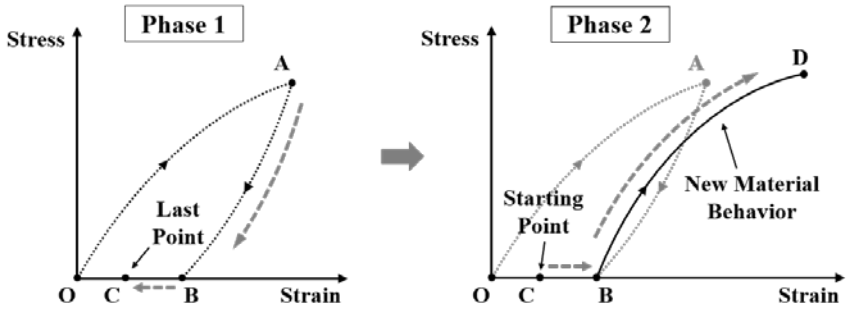

Fig. 11 – Transition of concrete stress-strain behavior from Phase 1 to Phase 2

© The 17th World Conference on Earthquake Engineering

4.4 Simulation result

Base shear-drift ratio responses of Column 1 and the stress-strain relationships of the concrete cylinder during the simulation are presented in Fig. 12. As the column was laterally loaded in Phase 1, the concrete cylinder experienced the compressive strain up to 0.41% with a peak stress of 33.9 MPa. The damage status of the concrete passively confined with the inactivated SMA wires is shown in Fig. 13 indicating that it experienced minor damages with very fine cracks. The experimental result obtained from the specimen was used to describe to uniaxial material behavior of the core concrete fibers. Fig. 14 presents stress-strain curves of two concrete fibers located at the top and bottom sections of the columns. It is shown that both concrete fibers followed the stress-strain envelope curve (Envelope 1) of the tested cylinder fairly well.

After the heating was applied to the SMA wires, the frame was again loaded up to 4% drift ratio in Phase 2. The lateral responses of Column 1 and stress-strain curve of the tested concrete cylinder are presented in Fig. 12. In Phase 2, Column 1 recorded a peak base shear of 885 kN at 1.8% drift ratio and continued to have the base shear of 829 kN when it reached a drift ratio of 4%. It is shown that the repaired column maintained its lateral capacity above 93% of its peak base shear (894 kN) achieved in Phase 1. In Fig. 12b, the repaired concrete recorded a peak stress of 31.7 MPa and a residual compressive stress of 22.2 MPa when it reached 1.26% axial strain in Phase 2. While being subjected to the large axial strain, the tested specimen experienced severe cracking and partial loss of concrete. However, the SMA confinement was able to induce the ductile behavior from the damage concrete and preventing its brittle failure. In Fig. 14, it is shown that the behaviors of the repaired concrete well followed the new material behavior (Envelope 2), and that smooth transition of the material behaviors was made the between Phase 1 and Phase 2.

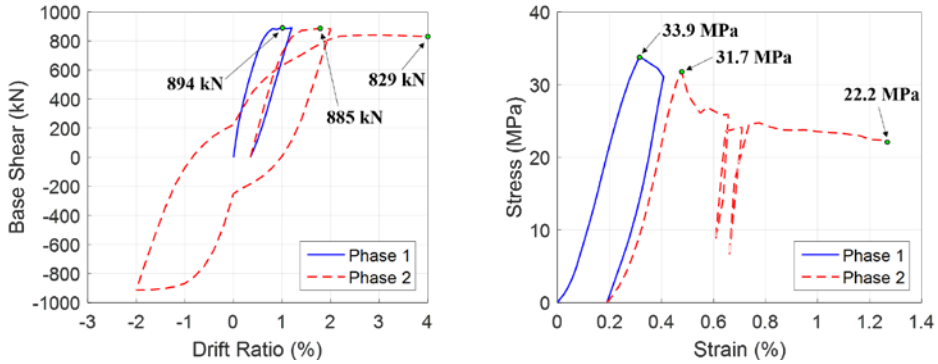

(a) (b)

Fig. 12 – Global and local responses of the RC column: (a) Base shear-drift ratio of Column 1 and (b) stress-strain behaviors of the concrete cylinder

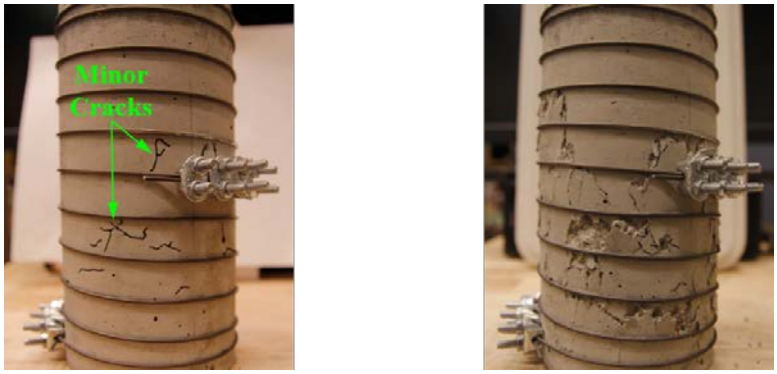

(a) (b)

Fig. 13 – Damage status of the tested concrete cylinder: (a) Phase 1 and (b) Phase 2

© The 17th World Conference on Earthquake Engineering

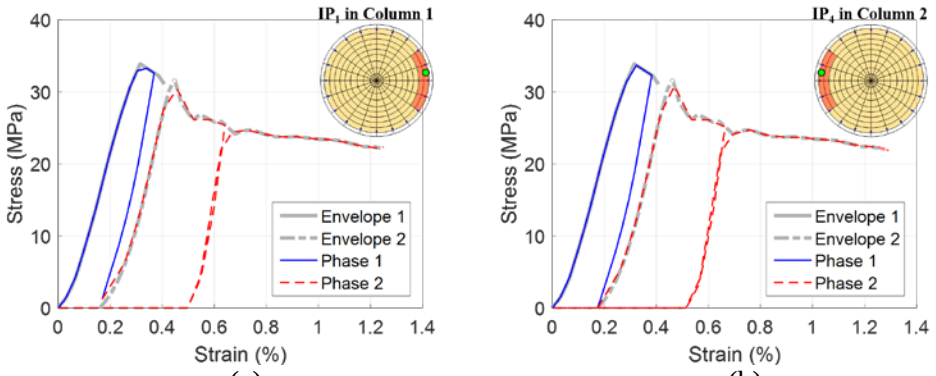

Fig. 14 – Stress-strain behaviors of concrete fibers: (a) IP_1 in Column 1 and (b) IP_4 in Column 2

6. Conclusions

A new framework, namely MTI simulation, was employed to explore the performance of SMA confinement for concrete with pre-existing damage. The important findings of the current study are summarized as follows:

- Within the new framework, the concrete behaviors under the complex conditions were well extracted from the physical specimen and incorporated as new material models in the simulations.
- After the SMA repair, the damaged concrete recorded the peak strength close to 98% of the unconfined concrete strength. The repaired concrete retained its compressive stress corresponding to 65% of its peak strength at the axial strain of 1.26%.
- The RC column repaired with the SMA confinement maintained 93% of its peak lateral force capacity at 4% drift ratio.

The simulation presented in this study focused on the behaviors of SMA confined concrete and the lateral response of the flexural RC frame. Further studies are needed to widen the application of MTI simulation to different types of materials, shear-dominant structural systems and more complex loading conditions combined with other various effects such as corrosion, fatigue or fire damage.

5. Acknowledgements

This research was funded by the National Science Foundation (NSF) through its Faculty Early Career Development (CAREER) program under Award No. 1055640, and the authors are grateful for the support.

6. References

[1] Khayat KH (1999): Workability, testing, and performance of self-consolidating concrete. *Materials Journal*, 96(3), 346-353.

[2] DesRoches R, McCormick J, Delemont M (2004): Cyclic properties of superelastic shape memory alloy wires and bars. *Journal of Structural Engineering*, 130(1), 38-46.

[3] Janke L, Czaderski C, Motavalli M, Ruth J (2005): Applications of shape memory alloys in civil engineering structures—overview, limits and new ideas. *Materials and Structures*, 38(5), 578-592.

[4] Graybeal BA (2007): Compressive behavior of ultra-high-performance fiber-reinforced concrete. *ACI Materials Journal*, 104(2), 146.

© The 17th World Conference on Earthquake Engineering

[5] Shin M, Andrawes B (2010): Experimental investigation of actively confined concrete using shape memory alloys. *Engineering Structures*, 32(3), 656-664.

[6] Cladera A, Weber B, Leinenbach C, Czaderski C, Shahverdi M, Motavalli M. (2014): Iron-based shape memory alloys for civil engineering structures: An overview. *Construction and building materials*, 63, 281-293.

[7] Czaderski C, Shahverdi M, Brönnimann R, Leinenbach C, Motavalli M (2014): Feasibility of iron-based shape memory alloy strips for prestressed strengthening of concrete structures. *Construction and Building Materials*, 56, 94-105.

[8] Sahmaran M, Li VC (2008): Durability of mechanically loaded engineered cementitious composites under highly alkaline environments. *Cement and Concrete Composites*, 30(2), 72-81.

[9] Fares H, Noumowe A, Remond S (2009): Self-consolidating concrete subjected to high temperature: mechanical and physicochemical properties. *Cement and Concrete Research*, 39(12), 1230-1238.

[10] Dommer K and Andrawes B (2012): Thermomechanical characterization of NiTiNb shape memory alloy for concrete active confinement applications. *Journal of Materials in Civil Engineering*, 24(10), 1274-1282.

[11] Alkaysi M, El-Tawil S, Liu Z, Hansen W (2016): Effects of silica powder and cement type on durability of ultra high performance concrete (UHPC). *Cement and Concrete Composites*, 66, 47-56.

[12] Zhao H, Andrawes B (2017): Mechanical properties of NiTiNb shape memory alloy subjected to a harsh corrosive environment. *Journal of Materials in Civil Engineering*, 29(3), 04016232.

[13] Molina FJ, Verzeletti G, Magonette G, Buchet PH, Geradin M (1999): Bi-directional pseudodynamic test of a full-size three-storey building. *Earthquake Engineering & Structural Dynamics*, 28(12), 1541-1566.

[14] Massone LM, Wallace JW (2004): Load-deformation responses of slender reinforced concrete walls. *ACI Structural Journal*, 101(1), 103-113.

[15] Wald F, da Silva LS, Moore DB, Lennon T, Chladna M, Santiago A, Beneš M,Borges L (2006): Experimental behaviour of a steel structure under natural fire. *Fire Safety Journal*, 41(7), 509-522.

[16] Panagiotou M, Restrepo JI, Conte JP (2010): Shake-table test of a full-scale 7-story building slice. Phase I: Rectangular wall. *Journal of Structural Engineering*, 137(6), 691-704.

[17] Echevarria A, Zaghi AE, Christenson R, Accorsi M (2015): CFFT bridge columns for multihazard resilience. *Journal of Structural Engineering*, 142(8), C4015002.

[18] Jung D, Andrawes B (2018): Application of new material testing integrated (MTI) simulation paradigm for studying concrete confinement. *Bulletin of Earthquake Engineering*, 1-21.

[19] Duerig TW, Melton KN, Stöckel D, Wayman CM (1990): *Engineering aspects of shape memory alloys*. Butterworth-Heinemann, London.

[20] Takanashi K, Udagawa K, Seki M, Okada T, Tanaka H (1975): Nonlinear earthquake response analysis of structures by a computer-actuator on-line system. *Bulletin of Earthquake Resistant Structure Research Center*, 8, 1-17.

[21] Takanashi K, Nakashima M (1987): Japanese activities on on-line testing. *Journal of Engineering Mechanics*, 113, 1014-1032.

[22] Mahin SA, Shing PB, Thewalt CR, Hanson RD (1989): Pseudodynamic test method—current status and future directions. *Journal of Structural Engineering*, 115, 2113-2128.

[23] Shing PB, Nakashima M, Bursi OS (1996): Application of pseudodynamic test method to structural research. *Earthquake Spectra*, 12, 29-56.

[24] Spacone E, Ciampi V, Filippou FC (1996): Mixed formulation of nonlinear beam finite element. *Computers & Structures*, 58, 71-83.

[25] Spacone E, Filippou FC, Taucer FF (1996): Fibre beam-column model for non-linear analysis of R/C frames: Part I. Formulation. *Earthquake Engineering & Structural Dynamics*, 25, 711-726.

© The 17th World Conference on Earthquake Engineering

[26] Nakata N, Spencer Jr, BF, Elnashai AS (2007): Multi-dimensional mixed-mode hybrid simulation control and applications. Newmark Structural Engineering Laboratory. University of Illinois at Urbana-Champaign, Illinois, USA.

[27] Dolce M, Cardone D, Marnetto R (2000): Implementation and testing of passive control devices based on shape memory alloys. *Earthquake Engineering & Structural Dynamics*, 29(7), 945-968.

[28] Saiidi MS, Wang H (2006): Exploratory study of seismic response of concrete columns with shape memory alloys reinforcement. *ACI Materials Journal*, 103(3), 436.

[29] Shin M, Andrawes B (2011): Lateral cyclic behavior of reinforced concrete columns retrofitted with shape memory spirals and FRP wraps. *Journal of Structural Engineering*, 137(11), 1282-1290.

[30] Shin M, Andrawes B (2012): Modeling and validation of RC columns seismically retrofitted using shape memory spiral. *In Proceeding of Structures Congress*, Chicago, IL.

[31] Choi E, Chung YS, Choi DH, DesRoches, R (2012): Seismic protection of lap-spliced RC columns using SMA wire jackets. *Magazine of Concrete Research*, 64(3), 239-252.

[32] Andrawes B, Shin M (2008): Seismic retrofit of bridge columns using innovative wrapping technique. *In Proceedings of Structures Congress*, Vancouver, Canada.

[33] Micelli F. Angiuli R, Corvaglia P, Aiello MA (2014): Passive and SMA-activated confinement of circular masonry columns with basalt and glass fibers composites. *Composites Part B: Engineering*, 67, 348-362.

[34] Jung D, Wilcoski J, Andrawes B (2018): Bidirectional shake table testing of RC columns retrofitted and repaired with shape memory alloy spirals. *Engineering Structures*, 160, 171-185.

[35] Gholampour A, Ozbakkaloglu T (2018): Understanding the compressive behavior of shape memory alloy (SMA)-confined normal-and high-strength concrete. *Composite Structures*, 202, 943-953.

[36] Giuffrè A, Pinto PE (1970): Reinforced concrete behavior under strong repeated loadings. *Giornale del Genio Civile*, 5, 391-408.

[37] Menengotto M, Pinto PE (1973): Method of analysis for cyclically loaded reinforced concrete plane frames including changes in geometry and nonelastic behavior of elements under combined normal force and bending. *In IABSE Symposium on Resistance and Ultimate Deformability of Structures Acted on by Well-Defined Repeated Loads*, Lisbon, Portugal.

[38] Shin M, Andrawes B (2011): Emergency repair of severely damaged reinforced concrete columns using active confinement with shape memory alloys. *Smart Materials and Structures*, 20(6), 065018.

[39] Popovics S (1973): A numerical approach to the complete stress-strain curve of concrete. *Cement and Concrete Research*, 3, 583-599.

[40] Chen Q (2015): Experimental testing and constitutive modeling of concrete confined with shape memory alloys. *Doctoral dissertation*, University of Illinois at Urbana-Champaign.

[41] Chen Q, Andrawes B (2017): Plasticity Modeling of Concrete Confined With NiTiNb Shape Memory Alloy Spirals. *Structures*, 11, 1-10.

© The 17th World Conference on Earthquake Engineering